

New Measurement of ^{165}Ho Neutron Capture Cross Section Data*

Su-Ya-La-Tu Zhang,^{1,2,†} Yong-Shun Huang,^{1,2} Wei Jiang,^{3,4} Rui-Rui Fan,^{3,4}
De-Xin Wang,^{1,2} Guo-Li,^{1,2} Dan-Dan Niu,^{1,2} and Mei-Rong Huang^{1,2}

¹Institute of Nuclear Physics, College of Physics and Electronic Information,
Inner Mongolia Minzu University, Tongliao 028000, Inner Mongolia, China.

²Inner Mongolia Joint Key Laboratory for Nuclear and Radiation Detection, Tongliao 028000, Inner Mongolia, China.

³Institute of High Energy Physics, Chinese Academy of Sciences, Beijing 100049, China.

⁴Spallation Neutron Source Science Center, Dongguan 523803, China

The neutron capture cross section data for ^{165}Ho were measured at the Back-streaming White neutron beam line (Back-n) of China Spallation Neutron Source (CSNS) using total energy detection systems, which comprise a set four C_6D_6 scintillator detectors coupled with pulse height weighting techniques. The resonance parameters were extracted using the multilevel, multichannel R-matrix code SAMMY, fitting the measured capture yields of the $^{165}\text{Ho}(\text{n},\gamma)$ reaction in the neutron energy range below 100 eV. Subsequently, the resonance region capture cross sections were reconstructed based on the obtained parameters. Additionally, the unresolved resonance average cross section of $^{165}\text{Ho}(\text{n},\gamma)$ reaction was determined relative to the standard ^{197}Au sample within the neutron energy range of 2 keV to 1 MeV. The experimental data were compared with the recommended nuclear data from the ENDF/B-VIII.0 library, as well as TALYS-1.9 code calculations. The comparison indicates that the measured $^{165}\text{Ho}(\text{n},\gamma)$ cross sections are in good agreements with these data. The present results are significant for evaluating the ^{165}Ho neutron capture cross section data, enhancing the quality of evaluated nuclear data libraries, and providing valuable guidance for nuclear theoretical models and nuclear astrophysical studies.

Keywords: Holmium, neutron capture reaction, cross section data, total energy detection principle, C_6D_6 scintillator detector, China Spallation Neutron Source.

I. INTRODUCTION

Nuclear data is used to describe the physical properties of atomic nuclei and their interactions. Neutron nuclear data plays key role in the research of fundamental nuclear physics and in the development of nuclear energy and nuclear technology [1, 2]. Neutron capture cross section data are extremely important for stellar nucleosynthesis of heavy elements, medical applications, radiation dosimetry, transmutation of nuclear waste, and advanced nuclear energy systems [3].

Many laboratories worldwide, including CERN n_TOF [4], Los Alamos National Laboratory DANCE [5], Karlsruhe [6], and GELINA [7] have developed two types of detection systems for the online measurement of neutron capture cross sections. These systems include the gamma-ray total energy and total absorption detectors. The total energy detection systems generally use a low efficient C_6D_6 scintillator detector, which is suitable for stable nuclide measurement of high cross-section and large samples. The total absorption detection systems often use BaF_2 crystal detector array with high energy resolution, good time resolution, low neutron sensitivity and high efficiency to carry out neutron capture measurement for small size sample, low cross section

and unstable radionuclides. The China Spallation Neutron Source (CSNS) [8] provide neutrons via high intensity 1.6 GeV proton beam bombarding on tungsten target. The back streaming neutron beam line (Back-n) facility is positioned in reverse direction of proton beam at the CSNS with a flight pass length of approximately 80 meters. Figure 1 shows the schematic view of the experimental setup of the CSNS Back-n. At present, five types of spectrometers are constructed for nuclear data measurement at Back-n, such as a set of four C_6D_6 detectors [9, 10] and a $4\pi \text{ BaF}_2$ detector array (called Gamma Total Absorption Facility II, GTAF-II) [11] for neutron capture measurement, a multilayer fast ionization chamber (FIXM) [12] for fission reaction measurement, a neutron total cross section detectors (NTOX) [13] for total cross section measurement, and a light-charged particle detectors (LPDA) [14] for light charged particle emission measurement. A detailed description of the spectrometers can be found in Refs [15].

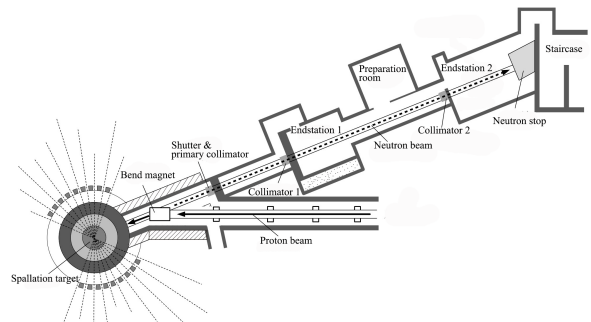


Fig. 1. (color online) Schematic view of the experimental setup of the CSNS Back-n [15].

* This work was supported by the National Natural Science Foundation of China (No.12465024,12365018,U2032146); Inner Mongolia National Science Foundation (No.2024ZD23,2024FX30,2023MS01005); Program for Innovative Research Team in Universities of Inner Mongolia Autonomous Region (NMGIRT2217); Program for Young Talents of Science and Technology in Universities of Inner Mongolia Autonomous Region (NJYT23109).

† Corresponding author.E-mail addresses: zsylt0416@163.com

The holmium has been proposed as a standard for neutron capture cross section measurements due to its suitable radioactive half-life and the large capture cross section at the first resonance peak for "saturation resonance" calibration [16–18]. Only a few experimental studies have been performed in the past for the low energy resonance region, and large discrepancies are observed between the reported data [19–22]. Therefore, much more neutron capture measurements of ^{165}Ho should be carried out for testing the accuracy of evaluated nuclear data and the available experimental data. This work present a new dataset of the $^{165}\text{Ho}(\text{n}, \gamma)^{166}\text{Ho}$ reaction in the neutron energy range from 1 eV to 1 MeV, which is measured by using the C_6D_6 detection system at the CSNS Back-n white neutron source. In the following sections, we outline the methods employed in the experiment and data analysis, discuss the reliability of results, and provide detailed information about the CERN ROOT code [23] relevant to this study.

II. METHODS

A. Measurement

In May 2022, measurement of the $^{165}\text{Ho}(\text{n}, \gamma)^{166}\text{Ho}$ reaction was performed at the CSNS Back-n experimental area (#ES2), where is located at flight path length of about 76 meters. The neutron beam was delivered at ES2 with about $6.92 \times 10^5 \text{ cm}^{-2} \text{ s}^{-1}$ neutrons per nominal pulse of 1.6×10^{13} protons in the energy range of 0.3 eV to 200 MeV of beam spots in $\phi 30$ mm. The neutron energy spectrum was determined using two different detectors, one being a Li-Si detector and the other being a calibrated fission chamber, which were based on the reactions of $^6\text{Li}(\text{n}, \text{t})$ and $^{235}\text{U}(\text{n}, \text{f})$, respectively [24, 25]. The neutron flux in the experiment was monitored by a silicon flux monitor (SiMon), consisting of a thin ^6LiF conversion layer and eight silicon detectors, approximately 20 meters upstream from the sample location. The γ -rays from the ^{165}Ho capture reaction were detected by a set of four C_6D_6 scintillators. The detectors were positioned approximately 17 cm from the target at an angle of 125 degrees relative to the neutron beam, as shown in figure 2. The characteristics of the samples used in this experiment, provided by the China Institute of Atomic Energy, are detailed in Table 1. A natural metallic holmium sample was employed to determine the neutron capture cross section of ^{165}Ho . A gold sample of the same dimensions as the holmium sample was utilized for measuring the neutron flux and normalizing the neutron capture data. Background measurements due to scattered neutrons and in-beam γ -rays were conducted using a lead sample. Additionally, an empty sample run was performed to evaluate the sample-independent background. Detector signals were recorded by the CSNS Back-n general-purpose Data Acquisition System [26], which operates at a sampling rate of 1 GS/s with 12-bit full-waveform digitizers. Data acquisition was triggered by the pickup signal from the proton beam. Total beam measurement time was 100 hours,

and the CERN ROOT code was utilized for offline analysis.

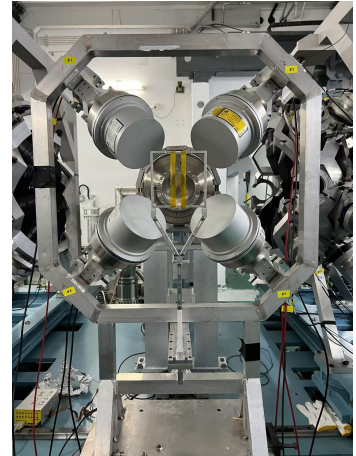


Fig. 2. (color online) The setup of the four C_6D_6 detectors in the measurement. The detectors were positioned approximately 17 cm from the target at an angle of 125 degrees relative to the neutron beam.

TABLE 1. Characteristic parameters of samples

Sample	Thickness (mm)	Diameter (mm)	Mass (mg)	Area desity (atom · b^{-1})
^{165}Ho	0.20	30	1243.32	6.42×10^{-4}
^{197}Au	0.10	30	1357.17	5.87×10^{-4}
^{nat}Pb	0.53	30	4249.75	1.75×10^{-3}
Empty holder				

B. Data analysis

The ^{nat}Pb sample data are parameterized as eq.(1) to evaluate the in-beam γ -rays and scattered-neutron background contributions for this experiment. The ^{165}Ho sample with the ^{181}Ta and ^{59}Co neutron filters are also performed and used to determine the normalization factors f_n and f_γ for B_n and B_γ components by matching the dips of the filtered spectra. The influence of the filters on in-beam γ -rays and neutrons is assessed carefully by analyzing the neutron flux and the energy distribution of the in-beam γ -rays [27]. Energy spectra of neutrons and γ -rays produced at spallation target are sampled randomly for the incident particle energy spectra of the GEANT4 Monte Carlo code [28], allowing for simulations both with and without filters. The counts of scattered neutrons and γ -rays are recorded at the detector position. The reduced attenuation factors for neutrons and γ -rays are found to be 0.92 and 0.68, respectively, which are applied as corrections to f_n and f_γ . Much more information of evaluation method used in this work can be found in Ref. [10].

$$B(E_n) = f_\gamma B_\gamma(E_n) + f_n B_n(E_n) \quad (1)$$

where the B_γ and B_n denote the background contribution of

117 the in-beam γ -rays and scattered neutrons, respectively, and
118 can be formulated as eqs. (2-3).

$$119 \quad B_\gamma(E_n) = b \times e^{-c/\sqrt{E_n}} + d \times e^{-e \times \sqrt{E_n}} + f \quad (2)$$

$$120 \quad 121 \quad B_n(E_n) = \frac{a}{\sqrt{E_n}} \quad (3)$$

122 The experimental neutron capture yield as a function of
123 neutron energy can be calculated as eq.(4)

$$124 \quad Y_{exp}(E_n) = \frac{1}{f_n} \frac{S(E_n) - B(E_n)}{\epsilon_c \times \Phi(E_n)} \quad (4)$$

125 where E_n is the incident neutron energy converted from the
126 neutron time-of-flight (TOF) spectra using the relativistic re-
127 lation. $S(E_n)$ is the count spectrum of the ^{165}Ho sample,
128 $B(E_n)$ is the evaluated background, $\Phi(E_n)$ is the neutron
129 flux spectrum. The normalization factor f_n , determined by
130 self-normalizing the measured capture yield of 4.9 eV res-
131 onance of ^{197}Au , accounts for the absolute incident neu-
132 tron flux. The ϵ_c is the detection efficiency of a capture
133 event. The total energy detection principle was used, com-
134 bining the above-mentioned C_6D_6 detection system with the
135 pulse height weighting technique (PHWT) [29], to achieve
136 the proportionality between the ϵ_c and the total γ -ray energy
137 (E_c) released in the capture event. Hence, $\epsilon_c = kE_c =$
138 $k(S_n + E_{cm})$, where S_n is the neutron separation energy (i.e.
139 6.24 MeV) of the compound nucleus, and E_{cm} is the center-
140 of-mass energy of the incident neutron. In the analysis of
141 the $^{165}\text{Ho}(n,\gamma)^{166}\text{Ho}$ measurement, the threshold established
142 are $E_{dep}^{min}=250$ keV and $E_{dep}^{max}=7$ MeV, corresponding to the
143 Compton edges for γ -ray energies of 124 keV and 6.75 MeV,
144 respectively. The weighted function (WF) as a 5th polyno-
145 mial function are fitted with Geant4 Monte Carlo code, sim-
146 ulating the C_6D_6 detector response for 27 different monoen-
147 ergetic γ -rays from 0.1 MeV to 10 MeV. This WF was then
148 applied to all the $S(E_n)$ and $B(E_n)$ spectra for following
149 data analysis.

150 The resonance shape analysis code SAMMY [30] was
151 used to fit the measured neutron capture yield calculated
152 by eq.(4). In the SAMMY code, the reaction cross section
153 data is described by a multi-level Reich-Moore formalism,
154 which only depends on the properties of the nuclear exci-
155 tation. This code takes into account all the experimental
156 conditions such as multiple interacting events, sample char-
157 acteristics, self-shielding, the broadening of resonances due
158 to thermal motion and experimental resolution of the CSNS
159 Back-n facility [31]. In the fitting process, the initial reso-
160 nance parameters were taken from the evaluated nuclear data
161 library ENDF/B-VIII.0 [33] and iteratively refined until con-
162 vergence. The resonance parameters, including resonance en-
163 ergy and capture kernels, were determined using SAMMY fits
164 within the resonance region up to 100 eV, where individual
165 neutron resonances were fitted with high precision. Based on
166 these resonance parameters, the resonance cross sections for
167 the $^{165}\text{Ho}(n, \gamma)^{166}\text{Ho}$ reaction were reconstructed. However,
168 resonance structures could not be adequately resolved beyond

169 approximately 100 eV due to the deterioration of experimen-
170 tal resolution and reduced event statistics as the neutron en-
171 ergy increased. Consequently, an averaged neutron capture
172 cross section was directly derived from the measured neutron
173 capture yield in unresolved resonance range using the formula
174 (5), where N_s represent the sample's areal density. In this
175 case, the measured capture yield was corrected for multiple
176 scattering and self-shielding effects through Geant4 code that
177 accounts for the sample composition, geometry, and both neu-
178 tron scattering and capture cross sections. Subsequently, the
179 ^{165}Ho neutron capture cross section was determined relative
180 to the standard ^{197}Au sample within the neutron energy range
181 of 2 keV to 1 MeV.

$$182 \quad \sigma_\gamma = \frac{Y_{exp}(E_n)}{N_s} \quad (5)$$

183 The systematic uncertainty for the measured cross sections
184 was determined from various sources. The energy depen-
185 dent neutron flux shape contributes an uncertainty of 4.5%
186 below 150 keV and 8.0% above this threshold. Additionally,
187 the uncertainty related to the normalization accounts for ap-
188 proximately 1%, while the calculation of PHWT introduces
189 a contribution of 3% to the overall uncertainties. Further-
190 more, the uncertainty from background subtraction using fil-
191 ters is about 8.6%, and an additional uncertainty of 0.01%
192 due to the sample impurities was also considered. The sum of
193 these components yields an overall systematic uncertainty of
194 10.2%(12.2%) for the capture cross section.

195 III. DATA RECORDS

196 For each neutron pulse, data from three different types of
197 detectors are simultaneously recorded and stored. One type is
198 a proton beam counter, monitored by the pick-up detector of
199 the Proton Synchrotron accelerator. The second type is a neu-
200 tron flux counter, composed of eight SiMon detectors. These
201 two data types are utilized for cross-validation and normaliza-
202 tion of various measurements. The third type of data includes
203 the event information for radiative neutron capture, recorded
204 by four C_6D_6 scintillator detectors. All the aforementioned
205 data are acquired using a fully digital data acquisition (DAQ)
206 system of the CSNS Back-n [26], with event-by-event con-
207 nectivity on the basis of CERN ROOT code. For each neu-
208 tron capture event, both of the deposited energy, represented
209 as a pulse height spectrum in the C_6D_6 detector, and TOF in-
210 formation of the incident neutrons are recorded. Table 2 lists
211 a comprehensive summary of the event information for all
212 samples utilized in the measurement. The data records are or-
213 ganized in Tree format according to the CERN ROOT version
214 5.34 and consist of two branch datasets: "NeuDataTree" and
215 "SiDataTree". "NeuDataTree" recorded data from four C_6D_6
216 detectors, including nine leaves: GPSsec (triggering time in
217 seconds), GPSnsec (triggering time in nanoseconds), T0id
218 (trigger T0 identification number), BCid (detector identifica-
219 tion number), Energy (neutron energy spectrum), Tof (time-
220 of-flight spectrum), Ph (pulse height spectrum), PeakValue

(pulse amplitude), and PeakPoint (pulse timing information). "SiDataTree", on the other hand, contained data from eight SiMon detectors, organized into six leaves: GPSsec (triggering time in seconds), GPSnsec (triggering time in nanoseconds), T0id (trigger T0 identification number), BCid(detector identification number), SiTof (time-of-flight spectrum), and SiPeakValue (pulse amplitude). This structured organization of data enables efficient storage and facilitates detailed analysis of time, energy, and spectral characteristics captured by the detectors.

TABLE 2. Summary of the event information for all samples.

Sample	Measurement time	Document Number	Number of Files
^{165}Ho	52h56m	15935,15955	1085
^{197}Au	5h16m	15927,15946	102
^{nat}Pb	9h41m	15931,15950	182
Empty holder	12h48m	15944,15956	190

All raw data described in this paper have been uploaded in the Science Data Bank. A direct link to the dataset is available at (<https://doi.org/10.57760/sciencedb.21041>).

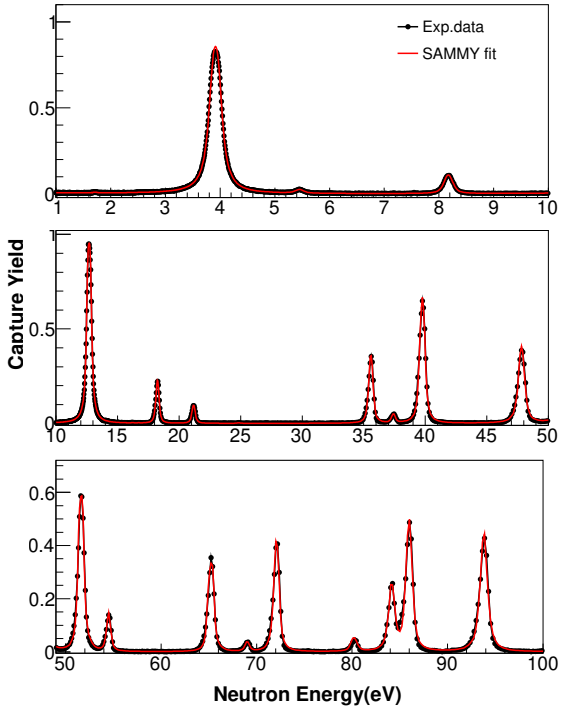


Fig. 3. (color online) SAMMY fits (red lines) to the measured capture yields (black circles) of $^{165}\text{Ho}(n, \gamma)^{166}\text{Ho}$ reaction.

IV. TECHNICAL VALIDATION

Figure 3 presents the SAMMY fits (red lines) compared to the measured capture yields (black circles) for the reaction $^{165}\text{Ho}(n, \gamma)^{166}\text{Ho}$ across neutron energy ranges below 100 eV. A good agreement is observed between measurement and SAMMY fits, both in terms of resonance energy and spectral shape. The resonance energies E_R , radiative width Γ_γ , neutron width Γ_n and capture kernels k ($k = g\Gamma_n\Gamma_\gamma/(\Gamma_n + \Gamma_\gamma)$,

g is the statistical factor) obtained in this study are compared with the data from the ENDF/B-VIII.0 library [33], as detailed in the Table 3. The experimental capture resonance parameters exhibit significant agreement with the ENDF/B-VIII.0 evaluations in the energy range below 100 eV. However, disparities are observed in the energy range between 100 eV and 2 keV, which can be ascribed to the degradation of experimental resolution function encountered at the CSNS Back-n facility during this measurement.

Figure 4 and 5 show the measured neutron capture cross sections obtained in this study, along with the calculated results from TALYS code version 1.9 [32] and the evaluated data derived from the ENDF/B-VIII.0 library [33]. The cross sections determined in this work are accurately reproduced by both the TALYS-1.9 calculations and the evaluated data across the full neutron energy range investigated. These results indicate that the experimental apparatus and data analysis methodologies have functioned effectively.

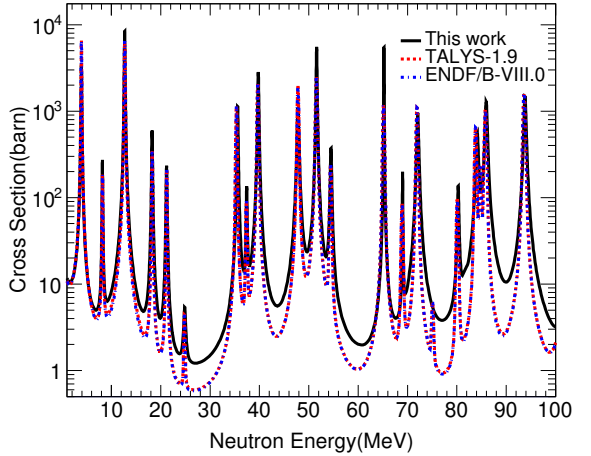


Fig. 4. (color online) Comparison of $^{165}\text{Ho}(n, \gamma)^{166}\text{Ho}$ cross sections, reconstructed from SAMMY resonance fits up to 100 eV neutron energy, with the calculations from TALYS code version 1.9 [32] and evaluated data derived from the ENDF/B-VIII [33].

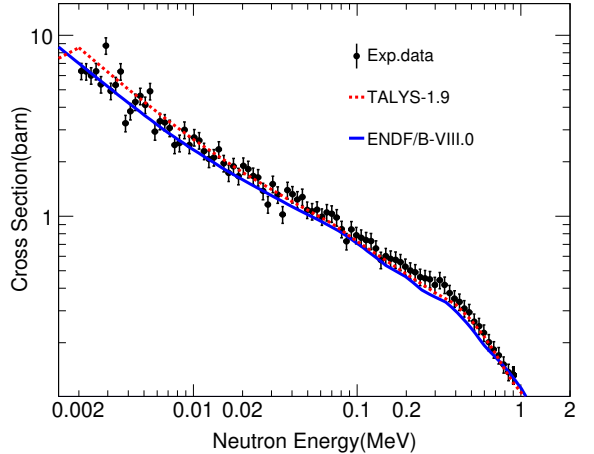


Fig. 5. (color online) Comparisons of the measured neutron capture cross section on ^{165}Ho of this work with the TALYS-1.9 calculations [32] and ENDF/B-VIII.0 evaluated data [33] in the 2 keV to 1 MeV.

TABLE 3. Resonance parameters up to 100 eV neutron energy for the ^{165}Ho (n, γ) cross sections.

J	This work				ENDF/B-VIII.0			
	$E_R(\text{eV})$	$\Gamma_n(\text{meV})$	$\Gamma_\gamma(\text{meV})$	k_R	$E_R(\text{eV})$	$\Gamma_n(\text{meV})$	$\Gamma_\gamma(\text{meV})$	k_R
4	3.91 ± 0.01	1.28 ± 0.01	129.10 ± 0.13	0.71 ± 0.01	3.91	2.13	85.70	1.17
3	8.17 ± 0.02	0.20 ± 0.01	98.66 ± 0.06	0.09 ± 0.01	8.17	0.19	90.30	0.08
4	12.68 ± 0.07	11.73 ± 0.15	122.82 ± 0.17	6.02 ± 0.04	12.69	10.31	84.00	5.17
3	18.24 ± 0.02	1.56 ± 0.18	159.76 ± 0.45	0.67 ± 0.06	18.25	0.95	78.10	0.41
4	21.16 ± 0.04	0.58 ± 0.02	167.16 ± 0.13	0.32 ± 0.01	21.19	0.52	68.00	0.29
3	28.38 ± 0.10	0.01 ± 0.01	16.50 ± 0.26	0.00 ± 0.00	24.79	0.02	84.00	0.01
3	35.58 ± 0.02	7.01 ± 0.08	184.08 ± 0.50	2.95 ± 0.03	35.33	8.69	73.60	3.40
4	37.41 ± 0.08	0.52 ± 0.02	162.36 ± 0.28	0.29 ± 0.01	37.36	0.50	83.00	0.28
4	39.76 ± 0.02	17.98 ± 0.02	193.14 ± 0.36	9.25 ± 0.01	39.67	16.80	88.00	7.94
3	47.82 ± 0.03	16.56 ± 0.16	329.52 ± 0.64	6.90 ± 0.06	47.80	28.23	92.00	9.45
3	51.57 ± 0.02	129.27 ± 0.12	95.13 ± 0.13	23.98 ± 0.03	51.55	56.57	85.00	14.86
4	54.50 ± 0.04	3.55 ± 0.53	241.76 ± 0.94	1.97 ± 0.19	54.42	2.40	84.00	1.31
4	65.23 ± 0.03	17.11 ± 0.15	360.22 ± 0.65	9.19 ± 0.07	65.15	18.67	77.00	8.45
4	69.01 ± 0.12	1.14 ± 0.06	269.18 ± 0.37	0.64 ± 0.03	68.91	1.10	89.00	0.61
4	72.12 ± 0.03	20.31 ± 0.03	218.50 ± 0.67	10.45 ± 0.02	71.93	20.44	74.00	9.01
3	-	-	-	-	75.08	0.09	84.00	0.04
4	80.30 ± 0.04	3.69 ± 0.08	1.80 ± 0.24	0.68 ± 0.03	80.10	1.55	82.00	0.85
4	-	-	-	-	83.80	13.51	67.00	6.32
3	84.15 ± 0.07	20.08 ± 0.05	397.93 ± 0.20	10.75 ± 0.02	84.73	5.60	84.00	2.30
3	85.96 ± 0.32	46.34 ± 0.68	293.48 ± 0.89	24.08 ± 0.17	85.80	37.37	84.00	11.32
4	93.80 ± 0.03	45.31 ± 0.33	515.19 ± 0.72	23.43 ± 0.13	93.63	73.78	79.00	21.46

260

V. USAGE NOTES

261 The dataset publication presents newly measured cross sec-
262 tions for the $^{165}\text{Ho}(n, \gamma)^{166}\text{Ho}$ reaction obtained with the
263 CSNS Back-n facility. Our objective is to comprehensively
264 document the data analysis procedures in a dedicated pub-
265 lication, thereby providing access to the neutron capture data
266 for both the nuclear physics community and researchers in re-
267 lated disciplines for future studies. This dataset has numerous
268 applications in nuclear physics, particularly in the following
269 areas:

270 (1) The spectroscopic information of heavy nuclei is chal-
271 lenging to obtain experimentally due to the rapid increase in
272 nuclear level density (NLD) with rising excitation energies.
273 To address this, statistical models provide a framework for
274 understanding the internal structure of these nuclei at higher
275 energies, relying on key parameters such as the NLD and the
276 γ -ray strength function (γ SF). These parameters are essen-
277 tial for a wide array of calculations in nuclear reactions, par-
278 ticularly in determining neutron capture reaction cross sec-
279 tions. The accuracy of these calculations is vital for evalua-
280 ting the reliability of nuclear models. In this context, the
281 case of ^{166}Ho , an odd-odd deformed nucleus, plays a signif-
282 icant role. The $^{165}\text{Ho}(n, \gamma)^{166}\text{Ho}$ neutron capture reaction
283 serves as a crucial tool for validating theoretical descriptions
284 of the NLD and γ SF. By examining this reaction, researchers
285 can test and refine the predictive power of nuclear models,
286 thereby enhancing our understanding of the underlying nu-
287 clear structure and reaction dynamics.

288 (2) The nucleosynthesis of elements heavier than iron is
289 considered one of the "11 Biggest Unsolved Mysteries in
290 Physics" that require urgent attention this century. Nuclear
291 astrophysicists generally agree that the slow neutron capture
292 process (s-process) and the rapid neutron capture process (r-
293 process) are the primary mechanisms responsible for the pro-
294 duction of these heavier elements. Holmium, an important
295 rare earth element, is primarily produced through explosive r-
296 process nucleosynthesis, with approximately 9% of its abun-
297 dance synthesised in the main s-process during the evolution
298 of intermediate-mass stars. The isotope ^{166}Ho is a significant
299 branching nucleus, characterised by a ground state half-life of
300 26.9 hours and an isomeric state (7^-) half-life of 1200 years,
301 primarily formed by the capture of a neutron by ^{165}Ho . Con-
302 sequently, the $^{165}\text{Ho}(n, \gamma)^{166}\text{Ho}$ reaction not only depletes
303 the abundance of ^{165}Ho but also influences the abundance
304 of ^{166}Ho and subsequent s-process nucleosynthesis products.
305 Therefore, this reaction cross section is critically important
306 for the study of nucleosynthesis in nuclear astrophysics.

307 (3) Holmium (Ho) has extensive applications in nu-
308 clear medicine, particularly the β^- and γ -emitting isotope
309 ^{166}Ho [$T_{1/2}=26.9$ h, $E_\beta = 1.77$ MeV (48%) and 1.85 (51%)
310 MeV, $E_\gamma = 81$ keV (6.7%)], which has been developed for ra-
311 diouclide therapy and single photon emission computed to-
312 mography (SPECT) imaging due to its favourable decay prop-
313 erties. The isotope ^{165}Ho is the only naturally stable isotope
314 of holmium (^{nat}Ho) and is used to produce ^{166}Ho through the
315 (n, γ) reaction. Accurate data on the neutron capture cross
316 section and resonance integral for the $^{165}\text{Ho}(n, \gamma)^{166}\text{Ho}$ re-

317 action are essential for evaluating neutron irradiation time,
 318 activity, and yield of ^{166}Ho produced in nuclear reactors.

319 VI. CODE AVAILABILITY

320 The publication of the dataset is accompanied by a soft-
 321 ware package based on CERN ROOT version 5.34/34 [23],
 322 which includes examples for reading the data, generating
 323 pulse height spectra of neutrons, performing background sub-
 324 traction, analyzing neutron resonances, and deriving neutron
 325 capture cross sections.

326 In the dataset, the neutron energy range from 0.2 eV to 2
 327 MeV was logarithmically divided into 3500 bins. The bin
 328 intervals and quantities can be reallocated according to the
 329 user's range of interest. Two classes, C_6D_6 Data and LiSi
 330 Data, are defined to read the corresponding data from the
 331 ROOT file. The TChain function is used to read all ROOT
 332 files under the same experimental conditions. For the C_6D_6
 333 data, the neutron energy thresholds were set to $E_{dep}^{min}=250$
 334 keV and $E_{dep}^{max}=7$ MeV, with the following detector param-
 335 eters:

336 $\text{C}_6\text{D}_6 : 1 \quad \text{C}_6\text{D}_6\text{Data}_1.\text{BCid} = 1, \quad \text{Min} : \text{bin} =$
 337 2822, $\text{Max} : \text{bin} = 78865;$
 338 $\text{C}_6\text{D}_6 : 2 \quad \text{C}_6\text{D}_6\text{Data}_1.\text{BCid} = 2, \quad \text{Min} : \text{bin} =$
 339 2822, $\text{Max} : \text{bin} = 78865;$
 340 $\text{C}_6\text{D}_6 : 3 \quad \text{C}_6\text{D}_6\text{Data}_1.\text{BCid} = 3, \quad \text{Min} : \text{bin} =$
 341 2807, $\text{Max} : \text{bin} = 78342;$
 342 $\text{C}_6\text{D}_6 : 4 \quad \text{C}_6\text{D}_6\text{Data}_1.\text{BCid} = 4, \quad \text{Min} : \text{bin} =$
 343 2890, $\text{Max} : \text{bin} = 80629;$

344 For the LiSi data, the signals from eight LiSi detectors were
 345 divided into two paths for storage, with the parameters being
 346 as follows:

347 $\text{LiSi} : 1 \quad \text{LiSiData}_1.\text{BCid} = 5$
 348 $\text{LiSi} : 1 \quad \text{LiSiData}_1.\text{BCid} = 6$

349 During the in-beam experiment, there was an issue with the
 350 second signal from the LiSi detector ($\text{LiSiData}_1.\text{BCid} =$
 351 6), so the first signal ($\text{LiSiData}_1.\text{BCid} = 5$) was chosen for
 352 data processing. The reaction between neutrons and ^6Li pri-
 353 marily generates helium nuclei (α) and tritium nuclei (T), re-

354 sulting in a bimodal structure in the energy spectrum. Due
 355 to the high energy of the T peak (2.73 MeV), saturation
 356 may occur during the experiment, leading to poor statisti-
 357 cal performance. Therefore, the α peak is selected as the
 358 effective neutron counting of the LiSi detector to determine
 359 the neutron flux. More detailed information about the data
 360 analysis code can be accessed as a notebook on the Sci-
 361 ence Data Bank, where the complete dataset for this work
 362 has been uploaded. A direct link to the dataset is available
 363 at: (<https://doi.org/10.57760/sciencedb.21041>).

364 ACKNOWLEDGEMENTS

365 Authors thanks to the efforts of the CSNS Back-n opera-
 366 tors for the skilled operation of the facility. We would like to
 367 express thanks to Hong-Wei Wang, Xi-Chao Ruan and Jing-
 368 Yu Tang for their helpful comments to the measurement. And
 369 also thank to Qi-Wen Fan for preparing the samples.

370 AUTHOR CONTRIBUTIONS STATEMENT

371 Su-Ya-La-Tu Zhang Conceptualization, Methodology,
 372 Writing-review & editing. Yong-Shun Huang Investigation,
 373 Data curation, Writing-original draft. Wei Jiang and Rui-
 374 Rui Fan Measurement, Methodology. De-Xin Wang Formal
 375 analysis. Guo-Li and Dan-Dan Niu Measurement. Mei-Rong
 376 Huang Writing- review & editing. All authors reviewed the
 377 manuscript.

378 COMPETING INTERESTS

379 The authors declare that they have no known competing
 380 financial interests or personal relationships that could have
 381 appeared to influence the work reported in this paper.

382 VII. REFERENCES

-
- 383 [1] G.Z. Gang, C.Y. Jing, Status and prospects of nuclear data 397 [5] I. Knapova, A. Couture, C. Fry, *et al.*, Photon strength
 384 development in China, Chin. Sci. Bull. 60 (32), 3087(2015). 398 functions, level densities, and isomeric ratio in ^{168}Er
 385 <https://doi.org/10.1360/N972015-00694> 399 from the radiative neutron capture measured at the
 386 [2] The n_TOF Collaboration, Nuclear data activities at the 400 DANCE facility, Phys. Rev. C 107(4), 044313(2023).
 387 n_TOF facility at CERN. Eur. Phys. J. Plus 131, 371(2016). 401 <https://doi.org/10.1103/PhysRevC.107.044313>
 388 <https://doi.org/10.1140/epjp/i2016-16371-4> 402 [6] K. Wisshak, F. Voss, F. Käppeler, *et al.*, Stellar neutron cap-
 389 [3] X.C. Ruan, Progress and prospect of neutron nuclear data mea- 403 ture cross sections of the Lu isotopes, Phys. Rev. C 73(1),
 390 surement. SCIENTIA SINICA Physica, Mechanica & Astro- 404 015807(2006). <https://doi.org/10.1103/PhysRevC.73.015807>
 391 nomica 50(5), 052002(2020). [https://doi.org/10.1360/SSPMA-2019-0231](https://doi.org/10.1360/SSPMA- 405 [7] C.J. Prokop, A. Couture, S. Jones, <i>et al.</i>, Mea-

 392 2019-0231) 406 surement of the $^{65}\text{Cu}(n, \gamma)$ cross section using the
 393 [4] C. Guerrero, J. Lerendegui-Marcó1, M. Paul, *et al.*, Neutron 407 Detector for Advanced Neutron Capture Experi-
 394 capture on the s-process branching point ^{171}Tm via time-of- 408 ments at LANL, Phys. Rev. C 99(5), 055809(2019).
 395 flight and activation. Phys. Rev. Lett. 125(142701), 1(2020) 409 <https://doi.org/10.1103/PhysRevC.99.055809>
 396 <https://doi.org/10.1103/PhysRevLett.125.142701>

- 410 [8] J. Tang, R. Liu, G. Zhang, *et al.*, Initial years' neutron-
411 induced cross-section measurements at the CSNS Back-n
412 white neutron source, Chin. Phys. C 45(6), 062001(2021).
413 <https://doi.org/10.1088/1674-1137/abf138>
- 414 [9] J. Ren, X. Ruan, W. Jiang, *et al.*, Neutron capture cross section
415 of ^{169}Tm measured at the CSNS Back-n facility in the energy
416 region from 30 to 300 keV, Chin. Phys. C 46(4), 044002(2022).
417 <https://doi.org/10.1088/1674-1137/ac4589>
- 418 [10] S. Zhang, G. Li, W. Jiang, *et al.*, Measurement
419 of the $^{159}\text{Tb}(n,\gamma)$ cross section at the CSNS
420 Back-n facility. Phys. Rev. C 107, 045809(2023).
421 <https://doi.org/10.1103/PhysRevC.107.045809>
- 422 [11] L. Xie, P. Cao, T. Yu, *et al.*, Real-time digital trigger sys-
423 tem for GTAF-II at CSNS Back-n white neutron source,
424 J. Inst. 16(10), P10029(2021). <https://doi.org/10.1088/1748-0221/16/10/P10029>
- 425 [12] Y. Yang, Z. Wen, Z. Han, *et al.*, A multi-cell fission cham-
426 ber for fission cross-section measurements at the Back-n white
427 neutron beam of CSNS, Nucl. Instrum. Methods Phys. Res. A
428 940, 486(2019). <https://doi.org/10.1016/j.nima.2019.06.014>
- 429 [13] J.M. Xue, S. Feng, Y.H. Chen, *et al.*, Measurement of the
430 neutron-induced total cross sections of ^{nat}Pb from 0.3 eV to
431 20 MeV on the Back-n at CSNS, Nucl. Sci. and Tech. 35,
432 18(2024). <https://doi.org/10.1007/s41365-024-01370-z>
- 433 [14] W. Jiang, H.Y. Bai, H.Y. Jiang, *et al.*, Application of a
434 silicon detector array in (n, lcp) reaction cross-section
435 measurements at the CSNS Back-n white neutron
436 source, Nucl. Instr. Methods A 973, 164126 (2020).
437 <https://doi.org/10.1016/j.nima.2020.164126>
- 438 [15] J.Y. Tang, Q. An, J.B. Bai, *et al.*, Back-n white neutron source
439 at CSNS and its applications, Nucl. Sci. and Tech. 32, 1(2021).
440 <https://doi.org/10.1007/s41365-021-00846-6>
- 441 [16] J.B. Czirr, M.L. Stelts, Measurement of the neutron cap-
442 ture cross section of holmium-165 and gold-197, Nucl. Sci.
443 and Eng. 52(3), 299(1973). <https://doi.org/10.13182/NSE73-A19477>
- 444 [17] R.L. Macklin, The ^{165}Ho (n,γ) Standard Cross Section
445 from 3 to 450 keV, Nucl. Sci. and Eng. 59(3), 231(1976).
446 <https://doi.org/10.13182/NSE76-A26821>
- 447 [18] A.D. Carlson, V.G. Pronyaev, D.L. Smith, *et al.*, Interna-
448 tional evaluation of neutron cross section standards, Nucl. Data
449 Sheets 110(12), 3215(2009). <https://doi.org/10.1016/j.nds.2009.11.001>
- 450 [19] F. Pogliano, A.C. Larsen, S. Goriely, *et al.*, Experi-
451 mentally constrained $^{165,166}\text{Ho}(n,\gamma)$ rates and implica-
452 tions for the s-process, Phys. Rev. C 107, 064614(2023).
453 <https://doi.org/10.1103/PhysRevC.107.064614>
- 454 [20] W.P. Poenitz, Fast neutron capture and activation cross sec-
455 tions, Natl. Bur. Stand.(US), Spec. Publ.(United States)
456 1975. <https://www.osti.gov/biblio/7364993>
- 457 [21] J.H. Gibbons, R.L. Macklin, P.D. Miller, *et al.*, Average
458 radiative capture cross sections for 7-to
459 170-keV neutrons, Phys. Rev. 122(1), 182(1961).
460 <https://doi.org/10.1103/PhysRev.122.182>
- 461 [22] J. Voignier, S. Joly, G. Grenier, Capture cross sections and
462 gamma-ray spectra from the interaction of 0.5-to 3.0-MeV neu-
463 trons with nuclei in the mass range A=45 to 238, Nucl. Sci. and
464 Eng. 112(1), 87(1992). <https://doi.org/10.13182/NSE91-92N>
- 465 [23] R. Brun, F. Rademakers, ROOT-An object oriented data
466 analysis framework, Nucl. Instr. Methods A 389, 81(1997).
467 [https://doi.org/10.1016/S0168-9002\(97\)00048-X](https://doi.org/10.1016/S0168-9002(97)00048-X)
- 468 [24] Q. Li, G. Luan, J. Bao, *et al.*, The ^6LiF -silicon detector array
469 developed for real-time neutron monitoring at white neutron
470 beam at CSNS, Nucl. Instr. Methods A 946, 162497(2019).
471 <https://doi.org/10.1016/j.nima.2019.162497>
- 472 [25] Y. Chen, G. Luan, J. Bao, *et al.*, Neutron energy spectrum mea-
473 surement of the Back-n white neutron source at CSNS, Eur.
474 Phys. J. A 55, 115 (2019). <https://doi.org/10.1140/epja/i2019-12808-1>
- 475 [26] Q. Wang, P. Cao, X. Qi, *et al.*, General-purpose read-
476 out electronics for white neutron source at China Spalla-
477 tion Neutron Source, Rev. Sci. Instrum. 89, 013511 (2018).
478 <https://doi.org/10.1063/1.5006346>
- 479 [27] J. Ren, X. Ruan, W. Jiang, *et al.*, Background study for (n,
480 γ) cross section measurements with C_6D_6 detectors at CSNS
481 Back-n, Nucl. Instrum. Methods Phys. Res. A 985, 164703
482 (2021). <https://doi.org/10.1016/j.nima.2020.164703>
- 483 [28] S. Agostinelli, J. Allison, K. Amako, *et al.*, GEANT4-a sim-
484 ulation toolkit, Nucl. Instrum. Methods Phys. Res. A 506, 250
485 (2003). [https://doi.org/10.1016/S0168-9002\(03\)01368-8](https://doi.org/10.1016/S0168-9002(03)01368-8)
- 486 [29] U. Abbondanno, G. Aerts, H. Alvarez, *et al.*, New
487 experimental validation of the pulse height weight-
488 ing technique for capture cross-section measurements,
489 Nucl. Instrum. Methods Phys. Res. A 521, 454 (2004).
490 <https://doi.org/10.1016/j.nima.2003.09.066>
- 491 [30] N.M. Larson, Updated user's guide for Sammy: Multilevel
492 R-matrix fits to neutron data using Bayes' equations[R]. Oak
493 Ridge National Lab.(ORNL), Oak Ridge, TN (United States),
494 2008. <https://doi.org/10.2172/941054>
- 495 [31] B. Jiang, J. Han, W. Jiang, *et al.*, Monte-Carlo calculations
496 of the energy resolution function with Geant4 for analyzing
497 the neutron capture cross section of ^{232}Th measured at CSNS
498 Back-n, Nucl. Instrum. Methods Phys. Res. A 1013, 165677
499 (2021). <https://doi.org/10.1016/j.nima.2021.165677>
- 500 [32] A.J. Koning, D. Rochman, J.C. Sublet, *et al.*, TENDL:
501 complete nuclear data library for innovative nuclear sci-
502 ence and technology[J]. Nucl. Data Sheets 155, 1(2019).
503 <https://doi.org/10.1016/j.nds.2019.01.002>
- 504 [33] M.B. Chadwick, M. Herman, P. Oblozinsky, *et al.*, ENDF/B-VII.1
505 nuclear data for science and technol-
506 ogy: cross sections, covariances, fission product yields
507 and decay data, Nucl. Data Sheets 112(12), 2887(2011).
508 <https://doi.org/10.1016/j.nds.2011.11.002>
- 509 [512]